S_2 Fluorescence and Ultrafast Relaxation Dynamics of the S_2 and S_1 States of a Ketocyanine Dye

Jahur A. Mondal, Hirendra N. Ghosh, T. Mukherjee, and Dipak K. Palit*

Radiation Chemistry and Chemical Dynamics Division, Bhabha Atomic Research Centre, Mumbai 400085, India

Received: February 17, 2005; In Final Form: May 26, 2005

Dynamics of the excited singlet (both the S_2 and S_1) states of a ketocyanine dye, namely, 2,5-bis[(2,3-dihydroindolyl)-propylene]−cyclopentanone (KCD), have been investigated in different kinds of media using steady-state absorption and emission as well as femtosecond transient absorption spectroscopic techniques. Steady-state fluorescence measurements, following photoexcitation of KCD to its second excited singlet state, reveal dual fluorescence (emission from both the S_2 and S_1 states) behavior. Although the intensity of the $S_2 \rightarrow S_0$ fluorescence is weaker than that of the $S_1 \rightarrow S_0$ fluorescence in solutions at room temperature (298 K), the former becomes as much as or more intense than the latter in rigid matrixes at 77 K. The lifetime of the S_2 state is short and varies between 0.2 and 0.6 ps in different solvents. After its creation, the S_2 state undergoes two simultaneous processes, namely, $S_2 \rightarrow S_0$ fluorescence and $S_2 \rightarrow S_1$ internal conversion. Time-resolved measurements reveal the presence of an ultrafast component in the decay dynamics of the S_1 state. A good correlation between the lifetime of this component and the longitudinal relaxation times (τ_L) of the solvents suggests that this component arises due to solvation in polar solvents. More significant evolution of the spectroscopic properties of the S_1 state in alcoholic solvents in the ultrafast time domain has been explained by the occurrence of the repositioning of the hydrogen bonds around the carbonyl group in the excited state of KCD. In 2,2,2-trifluoroethanol, a strongly hydrogen bond donating solvent, it has even been possible to establish the existence of two distinct forms of the S_1 state, namely, the non-hydrogen-bonded (or free) molecule and the hydrogen-bonded complex.

1. Introduction

In search of suitable polarity indicators, which should exhibit high fluorescence yield as well as the fluorescence maximum which should show extreme sensitivity to solvent polarity, Kessler and Wolfbeis synthesized a new class of dyes, known as ketocyanine dyes, which were N-substituted derivatives of 2,5-bis[propylene]−cyclopentanone.[1] In general ketocyanine dyes are α,β-unsaturated ketonic compounds, which are symmetrically substituted with amino-substituted donor groups at the terminal carbon atoms of the polyethylenic chains. Photophysical and spectroscopic properties of the ketocyanine dyes have been the subject of intensive investigations in recent years.[1−6] These dyes have been found to exhibit large positive solvatochromism, which has been explained in terms of the transition of the excited state from a polyene-like structure to a polymethine-like structure in highly polar solvents.[3] Hydrogen-bonding interaction with the alcoholic solvents is also expected to change the spectroscopic properties of these dyes significantly.

The pronounced solvent effects in both absorption and emission spectra of these dyes make them promising probes for monitoring micropolarity, hydrogen bond donating interaction, metal ion sensing, investigation of the cell membrane structures, and evaluating the microenvironmental characteristics of biochemical and biological systems.[1,2,5−10] Some of them are also used as laser dyes or photosensitizers and have found several industrial applications in photopolymer imaging systems.[11−13] Crown ether substituted derivatives of ketocyanine dyes are efficient fluorophores for alkaline earth cation recognition.[14]

Bagchi and co-workers made a systematic study on the solvation characteristics of several ketocyanine dyes using both the steady-state absorption and fluorescence as well as the time-resolved fluorescence measurements.[2] They showed that while nonspecific dipolar solvation is responsible for the solvatochromic properties of these dyes in aprotic solvents, specific interaction involving formation of an intermolecular hydrogen bond provides stronger solvatochromic behavior of these dyes in protic solvents. This group as well as Pivovarenko et al. have shown that the ketocyanine dyes form strong hydrogen-bonded complexes both in the ground state and in the excited state.[2a,6] However, fluorescence efficiency of these dyes is seen to be reduced significantly in protic solvents due to hydrogen-bonding interaction with the solvent.[4,6,10,15] Doroshenko and Pivovarenko studied the fluorescence behavior of differently N-substituted aminodibenzal derivatives of cyclopentanones.[4] They observed that the fluorescence yield of these dyes is strongly correlated with both the structure of the dye and the nature of the solvent, whether protic or aprotic. The fluorescence yield of each of these dyes is much lower in a protic solvent as compared to that in an aprotic solvent of comparable polarity. The yield depends on the N-substitution as well. For the N-substitution with structurally fixed alkyl amino groups, they observed significant solvent-induced fluorescence quenching in more polar solvents. This was explained by the increase of the internal conversion rate due to lowering of the energy gap between the S_1 and S_0 states with an increase in solvent polarity. However, in some

* Author to whom correspondence should be addressed. Telephone: 91-22-25595091. Fax: 91-22-25505151/25519613. E-mail: dkpalit@apsara.barc.ernet.in.

10.1021/jp0508498 CCC: $30.25
Published on Web 07/15/2005

CHART 1: Chemical Structure of KCD

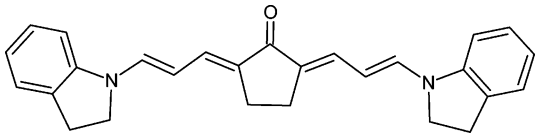

cases, fluorescence yield was seen to increase with increase in polarity of the aprotic solvents. This was explained by predicting lowering of the energy level of both the $S_1(\pi\pi^*)$ and $T_1(\pi\pi^*)$ states with respect to that of the $T_2(n\pi^*)$ state and hence reducing the rate of the thermally activated intersystem crossing process.[4]

Along with other ketocyanine dyes, Bagchi and co-workers also studied the photophysical and solvatochromic behavior of KCD (Chart 1).[2] One very interesting result regarding the photophysics of KCD reported by this group is that both the fluorescence quantum yield (ϕ_f) and the fluorescence lifetime (τ_f) of KCD, unlike in the case of many other ketocyanine dyes, increase with increasing solvent polarity.[2d] Additionally, in protic solvents, both ϕ_f and τ_f are remarkably higher than that in aprotic solvents of comparable polarity. This is also in contrast to the properties of other ketocyanine dyes.[2,4] Pramanik et al. also observed a blue shift of the absorption maximum of KCD in rigid matrixes at 77 K as compared to that at 298 K. They tried to explain this observation by proposing that, in solution, the excited state of the dye undergoes the twisted intramolecular charge-transfer (TICT) process, which is inhibited or slowed significantly in rigid matrixes.[2h] On the other hand, Doroshenko and Pivovarenko explained that the change of configuration due to cis−trans photoisomerization about one of the flexible C=C bonds may also provide another possible channel for the relaxation process of the dye in the excited state.[4] To reveal the possible role of different processes in the relaxation dynamics of the excited states of this class of dyes, we became motivated in investigation of the excited-state dynamics using ultrafast transient absorption spectroscopic technique. Of course the $S_2 \rightarrow S_0$ fluorescence and the dynamics of the S_2 state are the new aspects of the photophysics of the ketocyanine dye, which will be addressed for the first time here.

2. Experimental Section

KCD was a gift from Prof. Sanjib Bagchi of Burdwan University, India. The method of synthesis of this dye has been described elsewhere.[2a] All the solvents used were of spectroscopic grade (Spectrochem, India) and used as received without further purification.

Steady-state absorption spectra were recorded using a Shimadzu model UV-160A spectrophotometer. Fluorescence spectra were recorded using a Hitachi model 4010 spectrofluorimeter. The emission spectra were recorded using either 400 or 532 nm light for photoexcitation, and the samples were taken in a quartz tube of 4 mm diameter and put inside a quartz dewar flask. For measuring the fluorescence spectra in solid matrixes at liquid nitrogen temperature (77 K), the samples in the quartz tube were immersed into liquid nitrogen taken in the quartz dewar flask. The emission spectra were recorded both at room temperature and at 77 K with the same experimental arrangement.

Relaxation processes in the sub-500-ps time domain were measured using a femtosecond pump−probe transient absorption spectrometer,[16] which used a femtosecond Ti:sapphire laser system supplied by CDP-Avesta, Russia. The laser system consisted of a Ti:sapphire laser oscillator (model TISSA-50), which is pumped by a 5 W diode-pumped solid-state laser and produces laser pulses of 6 nJ energy at 800 nm. These pulses were amplified in an optical amplifier (model MPA-50) to generate 70 fs laser pulses of about 300 μJ energy at a repetition rate of 1 kHz using the chirped pulse amplification (CPA) technique. The optical amplifier consisted of a pulse stretcher, a multipass amplifier pumped by an intracavity frequency-doubled Nd:YAG laser (6 W, 1 kHz) and a pulse compressor. Pump pulses at 400 nm with an energy of 5 μJ/pulse were generated for excitation of the samples by frequency-doubling of one part of the 800 nm output of the amplifier in a 0.5 mm thick BBO crystal, and the other part of the amplifier output was used to generate the white light continuum (470−1000 nm) probe in a 2 mm thick sapphire plate. The direction of polarization of the pump beam was fixed at the magic angle. The sample solutions were kept flowing through a quartz cell of 1 mm path length. The probe beam was split into two equal parts, one of which passed through the excited zone of the sample to fall onto an integrating photodiode and the other part reached directly to another photodiode. For monitoring the decay dynamics at a particular wavelength, a region with 10 nm bandwidth was selected using a pair of interference filters placed in front of the photodiodes. The variation of the relative intensities of the two probe beams at different delay times with respect to the pump beam was monitored using the photodiodes coupled with two different boxcar integrators and then to an ADC and computer. The overall time resolution of the absorption spectrometer was determined to be about 120 fs by measuring the ultrafast growth of excited-state absorption (ESA) for tetraphenylprophyrin in benzene. The effects of temporal dispersion on the time-resolved spectra were also eliminated by determining the position of the zero delay between the pump and probe pulses by monitoring the growth of ESA of tetraphenylporphyrin in benzene at different wavelengths in the 470−1000 nm region. The temporal profiles recorded using different probe wavelengths were fitted with up to three exponentially decaying or growing components by iterative deconvolution method using a $sech^2$ type instrument response function with full width at half-maximum (fwhm) of 120 fs.

3. Results

3.1. Steady-State Absorption and Emission Studies. Ground-state absorption and steady-state fluorescence characteristics of KCD have been investigated in different kinds of solvents by Bagchi and co-workers. However, a brief discussion on a few important aspects of the steady-state spectroscopic properties of this dye is essential to understand the ultrafast dynamics of the excited state of KCD. Ground-state absorption and fluorescence spectra of KCD in six representative solvents are shown in Figure 1. The positions of the maxima of the absorption and fluorescence bands are given in Table 1. In methylcyclohexane (MCH) (dielectric constant, $\epsilon = 2.02$), the absorption maximum is at 470 nm (21 277 cm^{-1}) and the vibrational structures are well-resolved in the absorption spectrum. The absorption maximum undergoes a bathochromic shift with an increase in polarity of the aprotic solvents. However, the shift is much larger in a protic solvent of comparable polarity. For example, the absorption maxima are at 503 nm (19 880 cm^{-1}) and 534 nm (18 727 cm^{-1}) in acetonitrile ($\epsilon = 37.5$) and methanol ($\epsilon = 32.7$), respectively. In addition, the $S_1 \leftarrow S_0$ absorption band is significantly broadened in alcoholic solvents, as compared to those in MCH and acetonitrile. This lowest energy absorption ($S_1 \leftarrow S_0$) band arises due to $\pi\pi^*$ transition, involving an

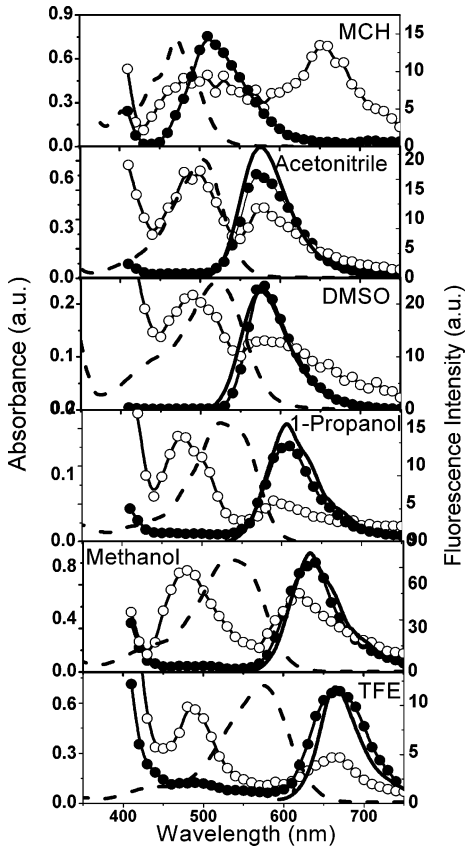

Figure 1. Ground-state absorption spectra (dashed line) and fluorescence spectra of KCD recorded in different solvents using 400 nm photoexcitation at room temperature (solid circles) and in solid matrixes at 77 K (open circles) and using 532 nm photoexcitation at room temperature (solid line).

intramolecular charge transfer (ICT) from the electron-donating indolyl group to the electron-accepting carbonyl group through the intervening conjugated system.[2a,3,17] The larger shift of the absorption maximum and larger width of the absorption band in methanol as compared to that in acetonitrile, which has polarity comparable to that of the former, suggests that the specific interaction between the dye and the solvent molecules via intermolecular hydrogen bonding is an important aspect, which controls the spectroscopic properties of the dye. This argument is also supported by the large bathochromic shift of the absorption maximum (17 422 cm^{-1}) in 2,2,2-trifluoroethanol (TFE), which is a strong hydrogen bond donating solvent. Bagchi and co-workers suggested the formation of a 1:1 hydrogen-bonded complex between the ground state of KCD and ethanol in benzene and ethyl acetate with equilibrium constants of 3.2 and 4.3, respectively.[2a] However, Pivovarenko et al. reported the existence of 1:1 and 1:2 type complexes in the excited state by identifying two new well-resolved bands in the fluorescence spectra of differently substituted ketocyanine dyes in the presence of low concentrations of alcohols (see later).[6] The absorption spectra of KCD in dimethylsulfoxide (DMSO), methanol, and TFE show the presence of a shoulder at ca. 450 nm, which is not very evident in those recorded in MCH and acetonitrile. This shoulder has arisen due to $S_2 \leftarrow S_0$ transition (see latter). In methanol and TFE, because of better stabilization of the lowest energy excited singlet (S_1) state, as compared to the next higher energy singlet (S_2) state, the energy gap between the S_2 and S_1 states increases and the two absorption bands are clearly resolved.

The steady-state fluorescence spectra of KCD have been recorded in several solvents of different kinds at room temperature (298 K) as well as in rigid matrixes at 77 K following photoexcitation using both 400 nm (to S_2 state) and 532 nm (to S_1 state) (Figure 1). Each of the fluorescence spectra recorded at room temperature using 532 nm light (in the case of MCH the excitation wavelength is 400 nm) consists of a single emission band with the emission maximum at 510 nm (19 608 cm^{-1}) in MCH, 570 nm (17 544 cm^{-1}) in acetonitrile and 580 nm (17 241 cm^{-1}) in DMSO. A large bathochromic shift of the fluorescence maximum due to an increase in solvent polarity suggests a larger dipole moment of the excited state than that of the ground state. The change in dipole moment ($\Delta\mu$) between the ground state and the fluorescing S_1 state of KCD has been determined to be 3.6 D.[2e] Here again, although methanol and acetonitrile are of comparable polarity, the fluorescence maximum in methanol (640 nm or 15 625 cm^{-1}) is red-shifted by 1919 cm^{-1} than that in acetonitrile. The fluorescence maximum occurs at 665 nm (15 038 cm^{-1}) in TFE. This fact further supports the specific interaction between KCD and protic solvents via formation of intermolecular hydrogen bond, which is expected to play a major role in the relaxation dynamics of the excited state due to larger separation of charge in this state.[2a,4]

We have found a new and important feature in the fluorescence spectra of KCD recorded in all kinds of solvents following photoexcitation of KCD at 400 nm, which excites the KCD molecules to its higher energy excited singlet state (S_2) (Figure 1). In addition to the $S_1 \rightarrow S_0$ emission band, we observe the appearance of a new emission band of very low intensity in the higher energy side of the former one. The presence of the higher energy band becomes more evident in the emission spectra recorded in solid matrixes at 77 K. For comparison of the features of the fluorescence spectra recorded following photoexcitation at 400 and 532 nm, we also recorded the emission spectrum at 77 K using 532 nm excitation (not shown in Figure 1). In this case, we observe a single emission band, which has the features (i.e. the shape and the position of the maximum) similar to that of the lower energy band in the emission spectrum recorded at 77 K using 400 nm light for photoexcitation. The position of the maximum of the higher energy emission band is nearly independent of the nature of the solvent but the relative intensity of this band as compared to that of the $S_1 \rightarrow S_0$ emission band varies depending on the nature of the solvent (Table 1). The relative intensities of the two fluorescence bands are sensitive to some extent to the quality of glass formation at 77K in different matrixes and the quality of the matrix was not possible to control to the extent that any quantitative ratio can be given. We assign the origin of the emission band, which has a maximum at ca. 490 nm (20 417 cm^{-1}), to the $S_2 \rightarrow S_0$ fluorescence.

In the emission spectra of KCD in MCH the S_2 and S_1 emission bands are closely spaced to each other with strong overlap. However, in acetonitrile, DMSO, and alcoholic solvents, they are well-resolved into two separate bands, since the maximum of the S_1 emission band is more red-shifted in these solvents. In MCH, in addition to the bands due to the S_2 and S_1 emissions, we observe the presence of another emission band in the lower energy side of the S_1 emission band. This band is assigned to the phosphorescence spectrum of KCD. The phosphorescence emission band is not observed in polar solvents (both aprotic and protic). Absence of phosphorescence emission in any of the polar solvents is possibly a consequence of change in the relative positions of the $S_1(\pi\pi^*)$, $T_1(\pi\pi^*)$, and $T_2(n\pi^*)$

TABLE 1: Absorption and Fluorescence Maxima and the Lifetimes of the S_2 State ($\tau(S_2)$) and the Relaxation Process (τ_R) Determined at Three Different Monitoring Wavelengths in Different Solvents[a]

solvents	η(cP), τ_L (ps)	λ_{max}(abs), nm ($S_1 \leftarrow S_0$)	λ_{max}(flu), nm $S_2 \rightarrow S_0$	λ_{max}(flu), nm $S_1 \rightarrow S_0$	$\tau(S_2)$, ps	τ_R(550nm), ps	τ_R(650nm), ps	τ_R(690/710nm), ps
MCH	−, −	470	480	510				
acetonitrile	0.34, 0.2	503	490	570	0.16	0.17	0.17	0.2
DMSO	2, 2.1	520	490	580	0.40	3.5	3.6	3.7
methanol	0.54, 9.2	532	480	640	0.25	6.5		12.5
ethanol	1.08, 27.4	528	475	630	0.30	17.3	22.3	27.5
1-propanol	2.0, 53	522	475	610	0.32	32.5	41	50.0
1-butanol	2.6, 120				0.40	25.1	27	40
1-pentanol	3.6, 151				0.5	40.5	42.2	62.1
1-octanol	6.33, −				0.6	54.0		
EG	16, 86				0.5	20		30
TFE	1.7, −	574	486	664	0.5		8.3	9.0

[a] τ_R represents the relaxation process of the S_1 state due to solvation (in aprotic solvents) and/or hydrogen-bond dynamics (in protic solvents). [b] Taken from ref 51. The viscosity values at 298 K. [c] Taken from refs 52 and 53.

levels in the singlet and triplet manifolds of energy levels with change in the polarity of the solvents.[4] In MCH, the position of the $T_2(n\pi^*)$ state lies below that of $S_1(\pi\pi^*)$ state and facilitates the intersystem crossing (ISC) process from the $S_1(\pi\pi^*)$ to the $T_2(n\pi^*)$ state following the El-Sayed rule.[18] However, in polar solvents, the $S_1(\pi\pi^*)$ state goes down below $T_2(n\pi^*)$ and makes the ISC process unfavorable, and also ISC between $S_1(\pi\pi^*)$ and $T_1(\pi\pi^*)$ states is not so efficient as a consequence of the same rule.[18]

Figure 1 reveals that the bandwidth (fwhm) of the $S_1 \rightarrow S_0$ emission spectrum of KCD recorded in the solid matrix of each of the alcoholic solvents is larger and the maximum is shifted toward the higher energy side as compared to that recorded at room temperature. In TFE, however, the positions of the maxima of the emission spectra recorded at room temperature and at 77 K appear at the same wavelength. We mentioned earlier that, in alcoholic solvents, the ground state of the dye molecule exists in equilibrium between the molecules, which are not hydrogen-bonded and those which form hydrogen-bonded complexes with the solvent molecules.[2a,6] The hydrogen-bonded complexes also may have different geometries and/or different stoichiometries. Hence, immediately after photoexcitation of KCD in alcohols, the excited states of both the non-hydrogen-bonded molecules and hydrogen-bonded complexes are created with the same composition as in the ground state. The larger bandwidth and hypsochromic shift of the maximum of the S_1 state emission band in solid glass matrixes of the normal alcohols, for instance, methanol and 1-propanol, as compared to those recorded in solution, suggests that emission in solid matrixes occurs from the excited states of both the non-hydrogen-bonded molecule as well as the hydrogen-bonded complexes before any kind of equilibration or reorganization of the solvent molecules takes place. It has been shown earlier that in many cases, a hydrogen bond between the solute and the solvent may dissociate easily and quickly following photoexcitation of the solute. Because of this, the two-dimensional hydrogen-bonded network structure of the solvent is disturbed as well.[19−21] In rigid matrixes, the motion of the solvent and solute molecules are nearly frozen and hence the alcohol molecules cannot reposition themselves around the newly created more polar solute to provide better stabilization of the excited state and the hydrogen-bonded network structure of the solvent. Hence emission takes place from a solute−solvent system, which consists of a nonequilibrated hydrogen-bonded network structure. However, in solution phase at room temperature, repositioning of the solvent molecules takes place in ultrafast time scale and emission takes place from the fully equilibrated hydrogen-bonded excited solute and the hydrogen-bond network structure of the solvent.

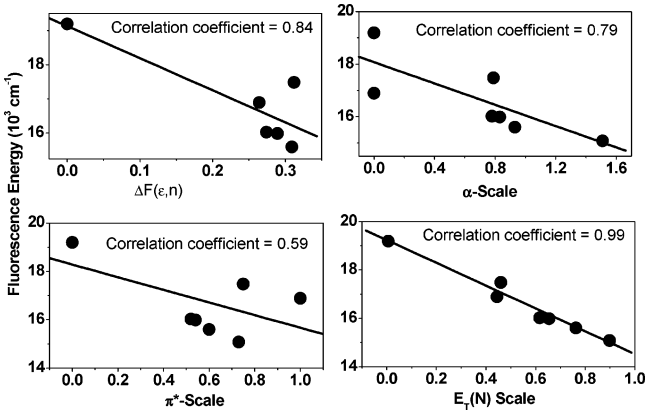

Figure 2. Correlation of fluorescence energy (corresponding to the maximum of fluorescence spectrum) with different solvent parameters. Fluorescence energy shows good linear correlation with $E_T(N)$ values of the solvents.

The cause of the solvent-assisted relaxation of the excited state of KCD can be predicted by correlating the fluorescence energy with the various measures of the solvent parameters, as shown in Figure 2. We find very poor correlation between the fluorescence energy and the reaction field parameter of the solvent, $\Delta F(\epsilon,n^2)$, which is defined by eq 1 and takes account of the influence of both the solvent dipolarity and solvent polarizability.

$$\Delta F(\epsilon,n^2) = \frac{\epsilon - 1}{2\epsilon + 1} - \frac{n^2 - 1}{2n^2 + 1} \qquad (1)$$

We have also shown the correlation between the fluorescence energy and the Kamlet−Taft's solvatochromic parameters, α and π^* of the solvents used here. The π^*-scale of solvent polarity is an empirical measure of solvation properties, which minimizes hydrogen-bonding effects.[22,23] Figure 2 also reveals that fluorescence energy is poorly correlated with this parameter. The fluorescence energy also shows little correlation with the empirical α-scale, which compares the hydrogen bond donating ability of the solvents.[23,24] In contrast, the fluorescence energies show good correlation with the $E_T(N)$ values of the solvents. The $E_T(N)$ scale is a popular measure of electronic state solvation and is known to be as much a measure of hydrogen bonding to the solvent as a measure of interaction with the solvent dipoles.[23,25] Breaking or formation of a hydrogen bond involves higher energy than the thermal energy, but a much lower energy than that in the case of a covalent bond. From this viewpoint, hydrogen-bond breaking and re-formation can be considered

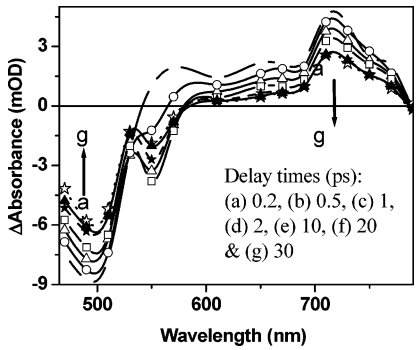

Figure 3. Time-resolved transient absorption spectra constructed at different delay times in a sub-30-ps time domain following photoexcitation of KCD in DMSO using 400 nm laser pulses.

as a specific solute−solvent interaction, resulting in the reorganization of the solvent molecules; i.e., it may be considered as one type of solvation dynamics (vide infra).[25]

3.2. Femtosecond Transient Absorption Studies. To delineate the aspects of participation of the higher energy excited states in the fluorescence emission as well as the role of hydrogen-bond dynamics in the relaxation processes of the excited states of KCD, the ultrafast dynamics of the excited states of KCD has been explored in different aprotic and protic solvents of varying polarities and viscosities using transient absorption spectroscopic technique with about 120 fs time resolution. For this purpose, 400 nm laser pulses of 70 fs duration have been used for excitation and the temporal profiles have been recorded at different wavelengths in the 470−1000 nm wavelength region at 20 nm intervals to construct the time-resolved transient absorption spectra. As discussed in section 3.1, one photon of 400 nm light excites a KCD molecule into its S_2 or higher electronic states (Figure 1).

Due to low solubility of KCD in MCH, the time-resolved absorption study could not be performed in this solvent but only in polar solvents. Figure 3 shows the time-resolved transient absorption spectra recorded following photoexcitation of KCD in DMSO. The spectrum constructed for 0.15 ps delay time after photoexcitation shows an ESA band in the 550−790 nm region with a maximum at ca. 710 nm, shoulders at 650 and 570 nm, and a band having negative absorbance values in the 470−500 nm region with a maximum at ca. 490 nm. Features of the time-resolved spectra evolve with an increase in delay time. Time-resolved spectra constructed in sub-30-ps time domain show that while both the negative absorption bands and the band due to ESA continue to decay, another negative absorption band with maximum at 550 nm is developing with an increase in delay time. Since the negative absorption band occurring in the 470−500 nm region overlaps with both the ground-state absorption band and the higher energy emission band occurring due to $S_2 \rightarrow S_0$ fluorescence (Figure 1), this band is expected to have a contribution from both the ground-state bleaching due to photoexcitation and the emission from the S_2 state, stimulated by the continuum probe light. The other negative absorption band with maximum at 550 nm overlaps with the lower energy emission band due to $S_1 \rightarrow S_0$ fluorescence (Figure 1), and hence it is assigned to the stimulated emission (SE) occurring from the S_1 state.

Temporal evolution of two negative absorption bands monitored at 490 and 550 nm as well as the ESA band at 710 nm are shown in Figure 4. The temporal profile monitored at 490 nm reveals a rapid rise of negative absorbance with the instrument-response time (∼120 fs). This rise is followed by a biexponential decay of negative absorbance. One of them is an

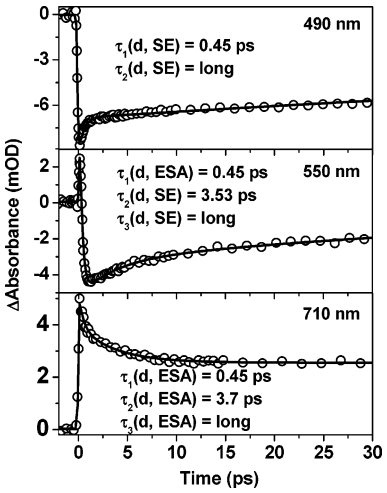

Figure 4. Temporal profiles of the transients monitored at three different wavelengths following photoexcitation of KCD in DMSO along with the best-fit function (solid lines). Lifetimes of the different components are also shown in the figure. The symbol "d" or "g" represents that the particular component is associated with either the decay or growth of either the excited-state absorption (ESA) or the stimulated emission (SE) at the monitoring wavelength.

ultrafast component with a lifetime of 0.45 ps, and another has a very long lifetime (>200 ps), which could not be determined accurately using our spectrometer, since it has the provision for delaying the probe pulse with respect to the pump pulse up to about 550 ps. The temporal profile recorded at 550 nm shows an initial appearance of ESA, but ESA decays quickly due to the growth of stimulated emission with a growth lifetime of 0.40 ps. This stimulated emission decays subsequently following a biexponential kinetics with one of the components having a lifetime of 3.53 ps and another having a long lifetime, which could not be measured here. The temporal profile for ESA monitored at 710 nm follows three exponential decay dynamics. Lifetimes of these components are given in the insets of Figure 4. Assignment of these lifetimes to different processes or species will be evident during the course of further discussion.

The presence of the ultrafast component with lifetime of 0.42 ± 0.03 ps in the temporal profile recorded at each of these wavelengths implicates the dynamics involving the S_2 state. At 490 nm, as we mentioned earlier, the negative absorption signal has contribution from both the ground-state bleach and the stimulated emission from the S_2 state; the ultrafast component of its decay represents a combined phenomena of bleach recovery and the decay of stimulated emission due to the same $S_2 \rightarrow S_0$ transition and obviously represents the lifetime of the S_2 state ($\tau(S_2)$). Since the growth lifetime of the stimulated emission monitored at 550 nm, which has been assigned to that due to the S_1 state, is nearly equal to $\tau(S_2)$, this component represents the $S_2 \rightarrow S_1$ internal conversion process by radiationless transition. However, the fluorescence lifetime of KCD in polar aprotic solvents, such as acetonitrile, has been reported to be about 1 ns.[2] Hence, the component with lifetime of 3.53 ps (we assign this as τ_R), which is associated with the decay of stimulated emission monitored at 550 nm, cannot be assigned to the lifetime of the S_1 state but to some kind of relaxation process happening in this state. The temporal profiles monitored at 650 and 710 nm, which represent the decay of ESA, also follow multiexponential dynamics, because of overlapping of the absorption bands due to both $S_n \leftarrow S_1$ and $S_n \leftarrow S_2$ transitions. The ultrafast component is assigned to the decay of the $S_n \leftarrow S_2$ absorption. We also observe the presence of a decay

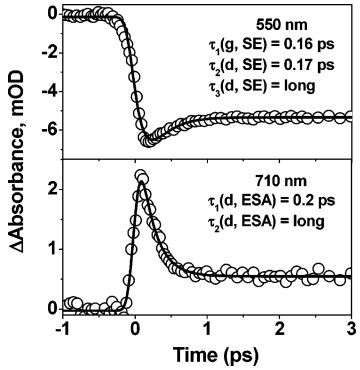

Figure 5. Temporal profiles of the transients monitored at 550 and 710 nm following photoexcitation of KCD in acetonitrile along with the best-fit function (solid lines). Lifetimes of the different components are shown in the figure. The symbol "d" or "g" represents that the particular component is associated with either the decay or growth of either the excited-state absorption (ESA) or the stimulated emission (SE) at the monitoring wavelength.

component of lifetime of 3.6 ± 0.1 ps, which is similar to that observed in the decay of stimulated emission from the S_1 state monitored at 550 nm ($\tau_R = 3.53$ ps) and represents the relaxation process taking place in the S_1 state.

To explore the origin of the component with lifetime, τ_R (3.6 ± 0.1 ps), we investigated the dynamics of the excited state of KCD in other aprotic and protic solvents with varying viscosities, solvation properties, and hydrogen-bonding abilities. Figure 5 shows the temporal evolution of the transient species produced following photoexcitation of KCD in acetonitrile monitored at 550 and 710 nm. The temporal profile monitored at 550 nm reveals the ultrafast rise of the stimulated emission intensity with lifetime of 0.16 ps, followed by its biexponential decay with the lifetimes of 0.17 ps and a long one. Following the same arguments as followed in the case of DMSO, the ultrafast component of the growth of stimulated emission with lifetime of 0.16 ps could be assigned to $\tau(S_2)$ and the component representing the decay of stimulated emission with lifetime of 0.17 ps can be assigned to τ_R. The temporal profile recorded at 710 nm also shows an ultrafast decay with lifetime of 0.2 ps and another decay component with a long lifetime (>200 ps). Hence, comparing the dynamics observed in acetonitrile and DMSO at the corresponding wavelengths, we observe that the lifetime of the S_2 state is about 0.18 ± 0.2 ps. However, this lifetime is very similar to τ_R, which is associated with the relaxation process, taking place in the S_1 state. Acetonitrile is also a polar aprotic solvent like DMSO, but the viscosity of acetonitrile ($\eta = 0.34$ cP) is about six times lower than that of DMSO ($\eta = 2.0$ cP). Longitudinal relaxation time, which is related to solvation time of the solvent, is also very short in the case of acetonitrile compared to that of DMSO (Table 1).

We have also investigated the dynamics of the excited states of KCD in other normal straight chain alcohols with varying length of the hydrocarbon chain, e.g. methanol to 1-octanol, as well as in ethylene glycol (EG). In the solvents of normal alcohol series, the properties such as viscosity and solvation time are varied systematically (Table 1). The spectral and temporal characteristics of the transient species produced in these alcoholic solvents have been observed to be very similar. Hence, we discuss the nature of the time-resolved spectra and the dynamical behavior of the transient species only in 1-propanol, as the representative one for this series of solvents. The lifetimes of the different species or processes, which have been determined by multiexponential fitting of the temporal profiles recorded at different wavelengths, are given in Table 1.

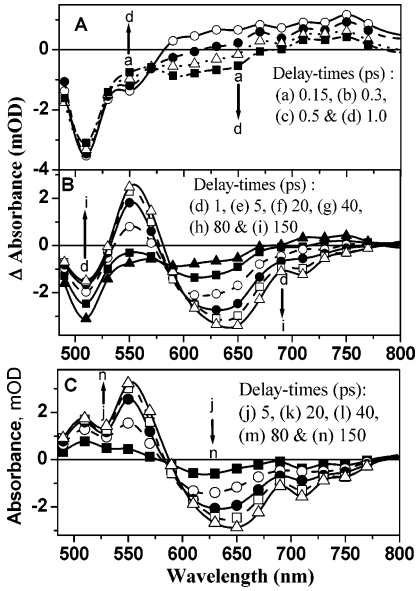

Figure 6. Time-resolved transient absorption spectra constructed in sub-1-ps (A) and sub-150-ps (B) time domains following photoexcitation of KCD in 1-propanol. (C) Corrected spectra after subtraction of the spectrum constructed for 1 ps delay time from each of the spectra shown in B.

Figure 6 shows the time-resolved spectra of the transient species produced upon photoexcitation of KCD in 1-propanol. The transient spectrum constructed for 0.15 ps delay time (Figure 6A) shows a negative absorption band in the 490−590 nm region and a broad ESA band in the 590−800 nm region. Following the arguments provided earlier, the occurrence of the negative absorption band could be assigned to two simultaneous processes, namely, the ground-state bleaching and the stimulated emission associated with the S_2 state (Figure 1). In the sub-1-ps time domain, the evolution of the time-resolved spectra shows a small decay (or partial recovery) of the negative absorption band as well as the decay of the ESA band in 590−800 nm, resulting in the development of another stimulated emission band in the 590−700 nm region. This evolution shows the presence of a temporary isobestic point at 570 nm. This suggests the involvement of two different states in the evolution of the time-resolved spectra shown in Figure 6A. One of them is appearing following the decay of the other. The decay of negative absorption in 490−570 nm is because of the $S_2 \rightarrow S_0$ transition, and the concomitant development of the stimulated emission band in the 590−650 nm region is assigned to the population of the S_1 state because of the $S_2 \rightarrow S_1$ internal conversion process. The decay of the ESA band in the 650−800 nm region also could be assigned to the same process. Figure 6B shows the evolution of the time-resolved spectra constructed in longer delay times ranging from 1 ps to 150 ps. We observe the development of the stimulated emission band in the 570−800 nm and an ESA band in the 530−570 nm region as well as the reduction of the negative absorption band in the 490−530 nm region. On increasing the delay time, the maximum of the stimulated emission band is shifted from 590 nm (observed at 1 ps delay time) to 650 nm (observed at 150 ps delay time). Since the fluorescence lifetime of KCD in 1-propanol has been reported to be very long (1.5 ns),[2g] the recovery of the negative absorption band in the 490−530 nm region cannot be assigned to the bleaching recovery due to repopulation of the ground state but possibly to the growth of an ESA band in the same region.[2] Hence the effect of ground-state bleaching on the transient spectra constructed at each delay time was corrected

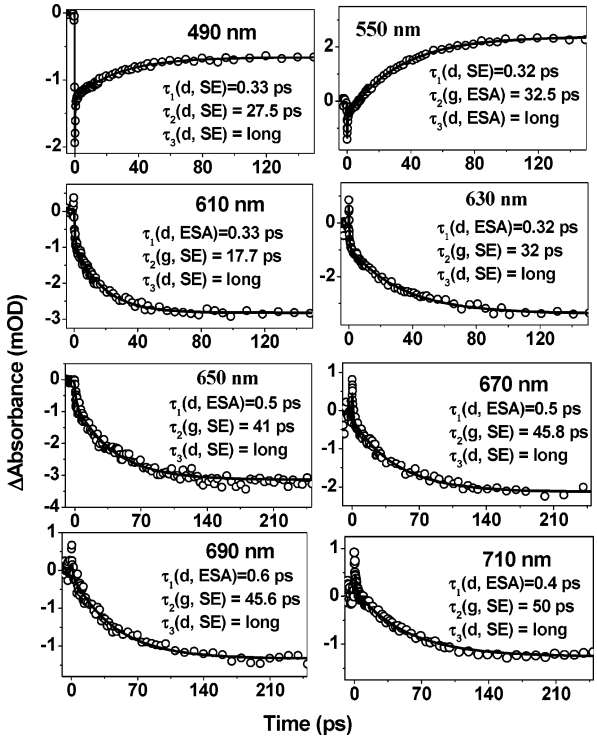

Figure 7. Temporal profiles of the transients monitored at different wavelengths following photoexcitation of KCD in 1-propanol along with the best-fit functions (solid lines). Lifetimes of different components are also shown in the figure. The symbol "d" or "g" represents that the particular component is associated with either the decay or growth of either the excited-state absorption (ESA) or the stimulated emission (SE) at the monitoring wavelength.

by subtracting the spectrum constructed for 1 ps from the respective spectrum constructed for the longer delay times to obtain the actual shape of the positive absorption band in the 490−570 nm region, and these corrected transient spectra are shown in Figure 6C. The ESA band appearing in the 490−560 nm region, which grows up to about 150 ps, is assigned to ESA due to the $S_n \leftarrow S_1$ transition and the negative absorption band in the 570−750 nm region to the stimulated emission from the S_1 state. The dynamic Stokes shift of the maximum of the time-resolved stimulated emission band from 590 to 650 nm cannot be assigned merely to solvation, since the stimulated emission band also grows simultaneously with increase in delay time.

Figure 7 shows the temporal evolution of the transient species in 1-propanol monitored at different wavelengths. At each of these wavelengths, the temporal profile could be best fitted by a three-exponential function, which represents growth and/or decay components, and the lifetimes of these components are shown in the insets of Figure 7. At 490 nm, the temporal profile reveals an ultrafast component of the decay of stimulated emission with a lifetime of 0.33 ps, which is the lifetime of the S_2 state, $\tau(S_2)$. The other component with lifetime of 27.5 ps, which is much shorter than the lifetime of the S_1 state (1.5 ns),[2g] should represent the relaxation process happening in the same state, i.e., τ_R. The long-lived component represents the long lifetime of the S_1 state. The lifetimes of the three components obtained by analyzing the temporal profile recorded at 550 nm reveal the same dynamics as those observed at 490 nm. The temporal profiles recorded in the 610−710 nm regions also reveal the presence of three components. Two of them represent the growth of stimulated emission, one of which is an ultrafast component for the formation of the S_1 state due to the $S_2 \rightarrow S_1$ internal conversion and another is due to the relaxation process

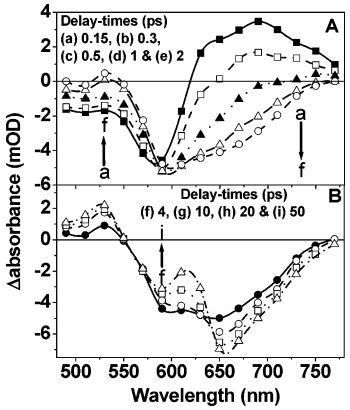

Figure 8. Time-resolved transient absorption spectra constructed in sub-5-ps (A) and sub-50-ps (B) time domains following photoexcitation of KCD in TFE.

happening in the S_1 state. The third and long-lived stimulated emission component represents the long lifetime of the S_1 state. However, as the monitoring wavelength changes from 610 to 690 nm, although the lifetime of the component arising due to the stimulated emission of S_2 remains the same within experimental error, that due to the relaxation process happening in the S_1 state, i.e., the value of τ_R, increases gradually.

Similar observations regarding the dynamics of the excited state of KCD have been made in other normal alcohols as well as in ethylene glycol. The average value of $\tau(S_2)$ and the values of τ_R determined at different monitoring wavelengths are given in Table 1. τ_R values show the same trend in all these solvents. τ_R increases as the monitoring wavelength changes from 610 to 690 nm. In addition, its value determined at a particular wavelength also increases with an increase in viscosity of the solvents. Hence, the spectral and dynamical characteristics of the transient species created due to photoexcitation of KCD in the S_2 sate represent a three-state process, namely, the decay of the S_2 state to a shorter lived unrelaxed singlet excited state (we assign this as the S_1' state) and conversion of the S_1' state to the energetically more stable, longer lived and relaxed S_1 state. Considering the structure of the molecule, the relaxation process observed to happen in the first excited singlet state can be assigned to either a change in configuration of the molecule, such as trans−cis isomerization taking place about one of the double bonds or twisting or rotation of the indolyl moiety followed by intramolecular charge transfer (i.e. TICT) process, or vibrational cooling of the nascent S_1' state to produce the S_1 state, or solvation and/or dynamics of a hydrogen bond (see latter).

To ensure which one of these processes is responsible for the relaxation process happening in the excited singlet state, the time-resolved absorptions of the transient species are compared in aprotic, protic, and a strongly hydrogen-bonding solvent, TFE. Figure 8 shows the time-resolved spectra of the transient species produced due to photoexcitation of KCD in TFE with 400 nm laser pulses, and the temporal dynamics monitored at different wavelengths are presented in Figure 9. The spectrum constructed for 0.15 ps delay time consists of two negative absorption bands in 490−530 and 530−620 nm regions and an ESA band in the 620−800 nm region. All these features are the characteristics of the S_2 state of KCD. Between the two negative absorption bands, the first one is assigned to the stimulated emission from the S_2 state, and the other one is to the bleaching of the ground state upon photoexcitation. The time-resolved spectra constructed at longer delay times (up to 2 ps) reveal the rapid decay of the stimulated emission band in

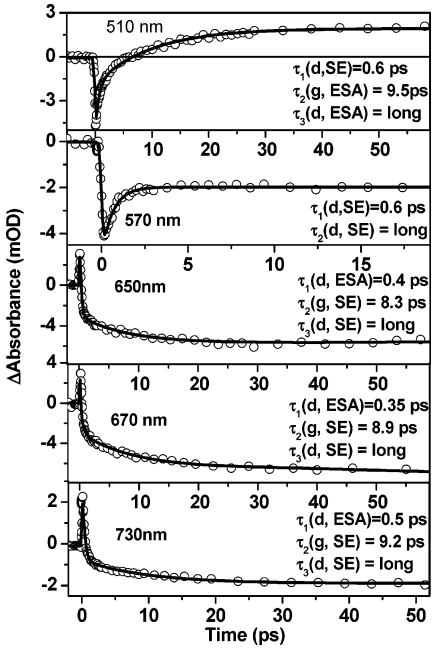

Figure 9. Temporal profiles of the transients monitored at different wavelengths following photoexcitation of KCD in TFE along with the best-fit functions (solid lines). Lifetimes of different components are also shown in the figure. The symbol "d" or "g" represents that the particular component is associated with either the decay or growth of either the excited-state absorption (ESA) or the stimulated emission (SE) at the monitoring wavelength.

the 490−530 nm region and the ESA band in the 620−800 nm region because of the $S_2 \rightarrow S_0$ radiative transition. However, the increase of negative absorbance in the 590−730 nm region indicates the development of another stimulated emission band with a maximum at 600 nm. Development of this emission band is less evident because of its overlap with that occurring due to bleaching. Upon further increase in delay time, we observe the decay of the stimulated emission band at 600 nm and development of another new stimulated emission band with maximum at 650 nm (Figure 8B). It is important to note that during these evolutions of the spectral characteristics, the bleaching band with maximum at 570 nm still survives and is recovered a little. Following the line of assignments of the different transient species in other solvents, the emission band with maximum at ca. 500, 600, and 650 nm are assigned to the S_2, S_1', and S_1 states, respectively. The lifetimes of the S_2 and S_1' states could be assigned to 0.5 ± 0.1 ps and 9.0 ± 0.5 ps, respectively. As in other solvents, the lifetime of the S_1 state is too long to measure here. However, unlike in other alcoholic solvents, the relaxation lifetimes (τ_R) in TFE increase marginally by changing the monitoring wavelengths from 650 to 730 nm (Figure 9).

4. Discussion

4.1. S_2 Fluorescence. Our steady-state fluorescence measurements establish the fact that KCD, upon photoexcitation to its S_2 state or higher excited singlet states, shows dual fluorescence behavior in all kinds of solvents. The S_2 state is weakly fluorescent in solution at room temperature, but the $S_2 \rightarrow S_0$ emission becomes relatively more intense in rigid matrixes at 77 K. The results of numerous experimental and theoretical studies have revealed that the anomalous $S_2 \rightarrow S_0$ fluorescence, in general, may appear if the $S_2 \rightarrow S_1$ radiationless internal conversion (IC) process is sufficiently slowed and depends mainly on the interplay of two factors, namely, the energy gap between the S_2 and S_1 levels (ΔE) and the density of levels in these two electronic states. The most important factor due to which the $S_2 \rightarrow S_0$ fluorescence becomes the reality is the large energy gap ($\Delta E > 3000$ cm^{-1}) between the S_2 and S_1 states, which reduces the vibronic coupling between these states and hence slows down the rate of $S_2 \rightarrow S_1$ IC process. The anomalous fluorescence from the S_2 state has been intensively studied in several classes of molecules, such as azulene and its derivatives ($\Delta E \sim 14\,000$ cm^{-1}),[26,27] thioketones ($\Delta E \sim 11\,000$ cm^{-1}),[28] substituted polyenes (e.g. diphenyloctatetraene ($\Delta E \sim 3100$ cm^{-1}) and β-carotene),[29,30] chlorophyls,[31] porphyrins ($\Delta E \sim 7000$ cm^{-1}),[32] and diphenyl- or triphenylmethane dyes ($\Delta E \sim 13\,000-16\,000$ cm^{-1}),[33] which are a few among many.[34] The energy gap between the S_2 and S_1 states of KCD has been calculated from the points of intersection between the fluorescence and absorption spectra, which are related to the corresponding transitions. These values are 3100, 3300, and 4000 cm^{-1} in MCH, DMSO, and methanol, respectively. Hence, in the case of KCD, the energy gap, ΔE, is quite moderate to observe the anomalous S_2 fluorescence.

Efficiency of the IC process, in addition to the energy gap between the S_2 and S_1 states, also depends on the extent of vibronic coupling between the S_2 and S_1 states. The intensity of S_2 fluorescence of KCD is significantly increased in rigid matrixes as compared to that in solution at room temperature. This suggests strong temperature dependence of the $S_2 \rightarrow S_1$ IC process, which is slowed significantly at 77 K. This happens because of a sparse level density of the accepting modes for the $S_2 \rightarrow S_1$ IC process. However, the excited levels of the active mode are thermally populated to a great extent, and hence the rate of the IC process increases significantly at 298 K compared to that at 77 K. So, the $S_2 \rightarrow S_1$ IC process in KCD is a thermally activated process. Diphenylacetylene is a unique polyene molecule, which show dual fluorescence in the gas phase despite a small energy gap between the S_2 and S_1 states ($\Delta E \sim 288$ cm^{-1}) due to the same reason.[35] Nemes et al. have shown that in the case of *N*-alkyl- or *N*-cycloalkyl-substituted molecules, the rate expression for IC process consists of two components—one is independent of temperature and the other is a thermally activated process.[36] The temperature-independent component of the IC process is associated with a direct process, in which the electronic energy is dissipated by a single vibrational mode. A strong temperature dependence of the IC process arises if vibrational coupling results in very low frequency of the vibronically active mode in the lower state.[37,38]

We mentioned earlier that the value of the S_2-S_1 energy gap is believed to be the principal factor determining the strength of the S_2 emission. However, the energy gap is not always the sole criterion for the slower rate of the $S_2 \rightarrow S_1$ internal conversion process. Symmetry restriction and spin multiplicity rules impose their own efficiency factors. We mentioned in the Introduction (section 1) that, in nonpolar solvents, KCD exists more likely in the "keto" form both in the ground and excited states. On the other hand, in polar solvents, due to the ICT character of the excited state, the structure of the excited state of the KCD can be represented as a mesomeric system having contributions from both the keto form and the zwitterionic (charge-transfer) form in aprotic solvents or "enol-like" form in protic solvents (Chart 2). Hence, following excitation the molecular system is changed from two isolated diene-like chromophores with five carbon atoms, which exists in the ground state, to a fully conjugated pentaene-like structure existing in the excited state. In the latter structure, the π-electronic conjugation is extended through the polymethine chain consisting of nine carbon atoms, as shown in Chart 2b.

CHART 2: (a) Zwitterion-like structure of KCD in polar aprotic solvents; (b) Enol-like form in protic solvents

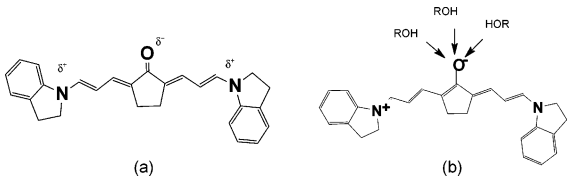

In polar protic solvents, the enol-like form is likely to exist even in the ground state as a consequence of strong intermolecular hydrogen-bonding interaction with the solvent.[4,6,15,16] Dual S_2 and S_1 fluorescence of polyenes with an intermediate number of conjugated bonds (five to nine double bonds) has been investigated under different conditions.[39] Short-chain polyenes, like diphenylhexatriene, are strongly S_1-fluorescent due to the long lifetime of the S_1 state.[40] For longer polyenes, like natural carotenoids, the fluorescence originating from a symmetry forbidden S_1-S_0 transition becomes weaker than the very weak S_2 fluorescence, possessing an ultrashort lifetime (0.2 ps).[30] Diphenyloctatetraene is another polyene which also shows an ultrafast emission originating from the S_2 state.[29] A decrease of the S_1 state emission intensity with increasing π-electron orbital length has been explained by an increased energy gap between the S_1 and S_2 states and the following decrease of the mixing (vibronic coupling) between these states. The energy gap between the S_1 and S_2 states of diphenyloctatetraene is as low as 3100 cm^{-1} in hexane. Despite the small energy gap ($\Delta E \sim 3000$ cm^{-1}) between the S_2 and S_1 states, the observation of S_2 fluorescence in long-chain polyenes has been justified by the symmetry-allowed $S_2(1^1B_u) \rightarrow S_0(1^1A_g)$ transition.[41,42] In the absence of any information available regarding the symmetry of the S_2 and S_1 states of KCD, we may possibly infer that the symmetry-allowed $S_2 \rightarrow S_0$ transition may be one of the important factors for observing S_2 fluorescence due to the polyene-like structure of the excited states. However, this postulation cannot explain the S_2 fluorescence of KCD in nonpolar solvent, MCH.

The above discussion suggests that the energy gap between the S_2 and S_1 energy levels, although not very large as those in azulene (14 000 cm^{-1}), TPM dyes (13 000−16 000 cm^{-1}), or thioketones (11 000 cm^{-1}), which are well-known for anomalous fluorescence emission, the S_2 emission in KCD with S_2-S_1 energy gap > 3100 cm^{-1} is not an improbable phenomenon. Support in favor of S_2 emission in KCD in different kinds of solvents has also been obtained from the time-resolved measurements. The investigation of the dynamics of the S_2 state has revealed a very short lifetime (0.2−0.6 ps depending on the nature of the solvent) of this state like the S_2 states of other polyenes, such as β-carotene.[43] The lifetime of the S_2 state is seen to increase with an increase in the viscosity of the solvents, though not in a very regular manner.

4.2. Relaxation Dynamics of the S_1' State. Upon photoexcitation of KCD directly to the S_2 state, the molecule undergoes two simultaneous processes, the $S_2 \rightarrow S_0$ fluorescence emission to come back to the ground state and the $S_2 \rightarrow S_1$ IC process to produce the S_1' state, which is in all-trans configuration as in the ground state.[2a] We mentioned earlier that the lifetime component, τ_R, could not be assigned to the decay of the S_1 state to come back to the S_0 state. Hence, we suggested that τ_R might be associated either with the change in conformation or cofiguration of the molecule in the excited state or vibrational cooling of S_1' state or solvation due to reorientation of the solvent molecules in aprotic solvents and/or hydrogen-bond

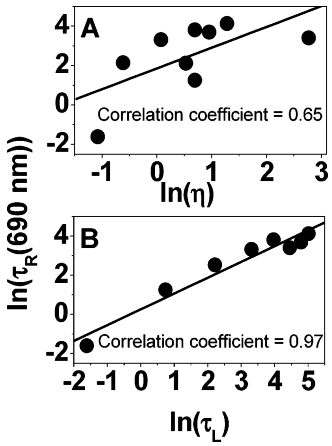

Figure 10. Plot of $\ln(\tau_R)$ vs $\ln(\eta)$ (A) and $\ln(\tau_R)$ vs $\ln(\tau_L)$ (B). The solid lines represent the best-fit linear function following eqs 3 and 5.

dynamics in alcoholic solvents. If the relaxation process is associated with any kind of conformational or configurational changes, τ_R should have a good correlation with the viscosity of the solvents. Kramers was the first to show that, in such cases, the solvent effect should be expressed through a "friction", which should be correlated with the lifetime as[44]

$$\tau_R = A\xi \exp(\Delta H/RT) \tag{2}$$

or

$$\ln(\tau_R) = \ln(\eta) + C + (\Delta H/RT) \tag{3}$$

where ξ represents the frictional force exerted by the solvent to retard the configurational changes of the solute molecule dissolved in it and is directly proportional to η, the viscosity of the solvent. If we assume that the Arrhenius parameter, ΔH, does not vary significantly due to change of solvents of the same class, we expect a linear relation between $\ln(\tau_R)$ and $\ln(\eta)$ (eq 3). If τ_R is associated with the trans−cis photoisomerization process or TICT process, it is a reasonable assumption that the value of ΔH should not be too different in different solvents of the same class, for example, alcohols. Figure 10 shows the plot of $\ln(\tau_R)$ vs $\ln(\eta)$ for the alcoholic solvents. We do not observe the linear correlation between these two parameters, as expected from eq 3. A qualitative examination of the data also reveals the lack of correlation of τ_R with solvent viscosities. For example, EG has substantially higher viscosity than that of 1-propanol and other alcohols of longer chain length, but the τ_R value in EG is shorter than that in these solvents (Table 1). Therefore, τ_R is not due to any kind of dynamics related to conformation or configurational changes in the excited state.

The longer lifetimes of the relaxation process and its significant dependence on viscosity excludes the possibility of its assignment to the solvent-assisted vibrational cooling process. In normal chain alcohols the value of τ_R increases from 12.5 ps in methanol to 62 ps in 1-octanol (Table 1). A solvent-assisted vibrational cooling process takes place typically in a time scale of a few hundreds of a femtosecond to 10 ps.[45−48] In addition, steady-state absorption and emission properties of KCD are very different in protic and aprotic solvents (section 3.1), and also, in time-resolved studies, the spectral evolution and the dynamics are remarkably different in aprotic and protic solvents (Figures 3 and 6). This indicates that τ_R should be associated with some other kind of processes in which specific interaction, e.g. hydrogen-bond between solute and solvent, plays an important

role in the relaxation dynamics of the S_1' state of KCD in alcoholic solvents. In hydrogen-bonding solvents, the Debye and/or longitudinal relaxation process is multiexponential and the longest component among the Debye dielectric (τ_D) or longitudinal relaxation (τ_L) times is generally assumed to be connected with the rate of hydrogen-bond reorganization in the solvent.[49,50] Hence, we made an attempt to correlate the relaxation dynamics with τ_L of the solvents.

In contrast to poor correlation of τ_R with the solvent viscosity, excellent correlation is found by equating the solvent friction, ξ, in eq 2, with τ_L of the solvent (eqs 4 and 5 and Figure 10B)

$$\tau_R = A(\tau_L) \exp(\Delta H/RT) \quad (4)$$

or

$$\ln(\tau_R) = \ln(\tau_L) + A + (\Delta H/RT) \quad (5)$$

The standard picture of nonspecific solvation dynamics assumes relatively weak intermolecular interactions. The interactions of the solute with each of the large number of solvent molecules are equally important and the dynamics involve motion along a collective coordinate involving motion of many solvent molecules. The barriers to these motions are small compared to thermal energies. However, the hydrogen bond dynamics can be thought as a bond-making or bond-breaking chemical reaction rather than merely a solvation process.[19−21,25] As we have observed in the case of KCD in TFE solvent, hydrogen-bond dynamics may be considered to be a conversion between two distinct states, namely, non-hydrogen-bonded and hydrogen-bonded. The barrier to hydrogen-bond breaking or forming is low, but not negligible as compared to thermal energies. In reality, hydrogen-bond dynamics can represent an intermediate situation between the nonspecific solvation and covalent bond breaking, considering the fact that it involves the exchange of energy, which is higher than the thermal energy but much lower than that of a covalent bond. The interaction of the solute with the single hydrogen-bonded solvent molecule is stronger than its interaction with other solvent molecules. However, the strength and dynamics of this interaction is not distinctly different from the hydrogen-bond interaction between solvent molecules. By considering the solute as the system and the hydrogen bond as part of the interaction with the bath, hydrogen-bond dynamics can be viewed as solvation dynamics; on the other hand, by considering the solute and bonded solvent molecules as the bath, hydrogen-bond dynamics can be viewed as a bond-breaking or -forming reaction.[25] Because of the intermediate strength of the hydrogen bond, it is not clear which picture is most appropriate. A comparison of the results of our experimental measurements in normal alcohols and TFE shows the features, which are characteristics of both. Whether the hydrogen-bond dynamics is a solvation process or a bond-breaking and bond-making process depends on the hydrogen bond donating ability of the solvent. In the present case, in normal alcohols, the wavelength-dependent growth of stimulated emission (or τ_R) representing the formation of the relaxed S_1 state because of repositioning of the hydrogen bond between the solute and solvent, leads us to consider it as merely a solvation process. On the other hand, the lack of dependence of τ_R on the wavelength of monitoring the growth of stimulated emission in TFE suggests that the hydrogen-bond dynamics investigated in this solvent can be thought of a bond-breaking and bond-making chemical reaction rather than a solvation process; i.e., the relaxation process in the singlet state can be described as a conversion of a non-hydrogen-bonded state (S_1') to a hydrogen-bonded state (S_1). In light of these arguments, the relaxation process of the S_1' state, which is associated with the time constant τ_R, is thus assigned to the repositioning of the hydrogen bonds around the excited solute molecule following perturbation due to photoexcitation.

Another important question to address in the context of the relaxation process of the singlet state of KCD is the higher fluorescence quantum yield and longer lifetime (a few nanoseconds) of the S_1 state in protic solvents as compared to those in aprotic solvents of comparable polarity. It is a very common observation that, due to strong intermolecular hydrogen bonds, the excited singlet state of ketonic compounds has a very short lifetime and very low fluorescence quantum yield as compared to those in aprotic solvents. Since, the stretching vibrations in hydrogen bonds act as efficient accepting modes for the radiationless energy, the rate of nonradiative IC process is very fast in protic solvents.[3,5] However, in KCD, the higher yield and longer lifetime of fluorescence in protic solvents possibly can be explained by the slower rate of the intersystem crossing process as a consequence of the relative positions of the nπ^* and $\pi\pi^*$ levels in the triplet manifold with respect to the lowest excited singlet (S_1) state. According to the El-Sayed rule, the rate of ISC process between the singlet and triplet states of the different orbital nature exceeds that of the identical orbital nature up to several orders of magnitude.[18]

In polar protic solvents, the lowest triplet (T_1) state of KCD has $\pi\pi^*$ character, but the nπ^* kind triplet state is the next higher triplet (T_2) state, which lies much higher than the $S_1(\pi\pi^*)$ state. Thus in polar protic solvent the efficient $S_1(\pi\pi^*) \rightarrow T_2(n\pi^*)$ is a thermally activated process. This situation, which reduces the rate of the ISC process, increases the yield and lifetime of fluorescence in more polar and protic solvents.

5. Conclusion

In this paper, we report, for the first time, the phenomenon of S_2 fluorescence in a ketocynaine dye as well as the time-resolved study of the ultrafast dynamics of the S_2 and S_1 states using femtosecond transient absorption spectroscopic technique. KCD shows dual fluorescence (emission from both the S_2 and S_1 states) behavior in all kinds of solvents. Although S_2 fluorescence is weak in solution at room temperature, its intensity increases significantly in rigid matrixes at 77 K. The phenomenon of S_2 fluorescence has been explained by the larger energy gap between the S_2 and S_1 states (ΔE varies between 3100 and 4000 cm^{-1} in different solvents) and sparse level density of the active modes for $S_2 \rightarrow S_1$ IC. We also observe the ultrafast dynamics of the S_1 state due to solvation in aprotic solvents or hydrogen-bond dynamics in alcoholic solvents.

Acknowledgment. We gratefully acknowledge Prof. S. Bagchi of the University of Burdwan for his gift of the dye. The authors are also grateful to Dr. Dilip Maiti of Radiation Chemistry and Chemical Dynamics, BARC, for fruitful discussion.

References and Notes

(1) Kessler, M. A.; Wolfbeis, O. S.; *Spectrochim. Acta* **1991**, *47A*, 187.
(2) (a) Banerjee, D.; Laha, A. K.; Bagchi, S. *Indian J. Chem.* **1995**, *34A*, 94. (b) Banerjee, D.; Laha, A. K.; Bagchi, S. *J. Photochem. Photobiol. A: Chem.* **1995**, *85*, 153. (c) Banerjee, D.; Mondal, S.; Ghosh, S.; Bagchi, S. *J. Photochem. Photobiol. A: Chem.* **1995**, *90*, 171. (d) Banerjee, D.; Das, P. K.; Mondal, S.; Ghosh, S.; Bagchi, S. *J. Photochem. Photobiol., A* **1996**, *98*, 183. (e) Banerjee, D.; Bagchi, S. *J. Photochem. Photobiol., A* **1996**, *101*, 57. (f) Pramanik, R.; Das, P. K.; Bagchi, S. *J. Photochem. Photobiol., A* **1999**, *124*, 135. (g) Pramanik, R.; Das, P. K.; Bagchi, S. *Phys. Chem. Chem. Phys.* **2000**, *2*, 4307. (h) Pramanik, R.; Das, P. K.; Banerjee,

D.; Bagchi, S. *Chem. Phys. Lett.* **2001**, *341*, 507. (i) Shannigrahi, M.; Pramanik, R.; Bagchi, S. *Spectrochim. Acta* **2003**, *59A*, 2921. (j) Das, P. K.; Pramanik, R.; Banerjee, D.; Bagchi, S. *Spectrochim. Acta* **2000**, *56A*, 2763.

(3) Marcotte, N.; Fery-Forgues, S. *J. Photochem. Photobiol., A* **2000**, *130*, 133.

(4) Doroshenko, A. O.; Pivovarenko, V. G. *J. Photochem. Photobiol., A* **2003**, *156*, 55.

(5) Doroshenko, A. O.; Bilokin, M. D.; Pivovarenko, V. G. *J. Photochem. Photobiol., A* **2004**, *163*, 95.

(6) Pivovarenko, V. G.; Klueva, A. V.; Doroshenko, A. O.; Demchenko, A. P. *Chem. Phys. Lett*. **2000**, *325*, 389.

(7) Reichardt, C. *Chem. Rev*. **1994**, *94*, 2319.

(8) Doroshenko, A. O.; Grigorovich, A. V.; Posokhov, E. A.; Pivovarenko, V. G.; Demchenko, A. P. *J. Mol. Eng.* **1999**, *8*, 199.

(9) Doroshenko, A. O.; Sychevskaya, L. B.; Grygorovych, A. V.; Pivovarenko, V. G. *J. Fluoresc.* **2002**, *12*, 451.

(10) Rurack, K.; Dekhtyar, M. L.; Bricks, J. L.; Resch-Genger, U.; Rettig, W. *J. Phys. Chem. A* **1999**, *103*, 9626.

(11) Barnabas, M. V.; Liu, A.; Trifanac, A. D.; Krougauz, V. V.; Chang, C. T. *J. Phys. Chem*. **1992**, *96*, 212.

(12) Chambers, W. J.; Eaton, D. F. *J. Imaging Sci*. **1986**, *13*, 230.

(13) Baun, M. D.; Henry, C. P. *Ger. Offen*. 2,133,315, Jan. 13, 1972; U.S. Pat. Appl. 53,686, Jul. 09, 1970.

(14) Marcotte, N.; Ferry-Fogues, S.; Lavabre, D.; Marquet, S.; Pivovarenko, V. G. *J. Phys. Chem*. **1999**, *103*, 3163.

(15) (a) Rurack, K.; Dekhtyar, M. L.; Birks, J. L.; Resch-Genger, U.; Rettig, W. *J. Phys. Chem. A* **1999**, *103*, 9626. (b) Rurack, K.; Birks, J. L.; Reck, G.; Radeglia, R.; Resch-Genger, U. *J. Phys. Chem. A* **2000**, *104*, 3087.

(16) Mondal, J. A.; Ramakrishna, G.; Singh, A. K.; Ghosh, H. N.; Mariappan, M.; Maiya, B. G.; Mukherjee, T.; Palit, D. K. *J. Phys. Chem. A* **2004**. *108*, 7843.

(17) Fery-Fogues, S.; Delavaux-Nicot, B.; Lavabre, D.; Rurack, K. *J. Photochem. Photobiol., A* **2003**, *155*, 107.

(18) El-Sayed, M. A. *J. Phys. Chem*. **1963**, *38*, 2834.

(19) Chudoba, C.; Nibbering, E. T. J.; Elsaesser, T. *Phys. Rev. Lett.* **1998**, *81*, 3010.

(20) Chudoba, C.; Nibbering, E. T. J.; Elsaesser, T. *J. Phys. Chem. A* **1999**, *103*, 5625.

(21) Palit, D. K.; Zhang, T.; Kumazaki, S.; Yoshihara, K. *J. Phys. Chem. A* **2003**, *107*, 10788.

(22) (a) Kamlet, J. M.; Abboud, J. L.; Taft, R. W. *J. Am. Chem. Soc.* **1977**, *99*, 6027. (b) Kamlet, J. M.; Abboud, J. L.; Taft, R. W. *Prog. Phys. Org. Chem.* **1981**, *13*, 485.

(23) Reichardt, C. *Solvents and Solvent Effects in Organic Chemistry*; VCH Verlagsgesellschaft GmbH: Weinheim, Germany, 1990.

(24) Kamlet, J. M.; Dickension. C.; Taft, R. W. *Chem. Phys. Lett.* **1981**, *77*, 69.

(25) Benigno, A. J.; Ahmed, E.; Berg, M. *J. Chem. Phys.* **1996**, *104*, 7382.

(26) Beer, M.; Longuet-Higgins, H. C. *J. Chem. Phys*. **1955**, *23*, 1390.

(27) Murata, S.; Iwanaga, C.; Toda, T.; Kokubun, H. *Chem. Phys. Lett.* **1972**, *13*. 101.

(28) Maciejewski, A.; Steer, R. P. *Chem. Rev*. **2003**, *93*, 67

(29) Bachilo, S. M.; Gillbro, T. *Chem. Phys. Lett.* **1994**, *218*, 557.

(30) (a) Bondavev, S. L.; Bachilo, S. M.; Dvornickov, S. S.; Tikhomirov, S. A. *J. Photochem. Photobiol., A* **1989**, *46*, 315. (b) Gilbro, T.; Cogdell, R. J. *Chem. Phys. Lett*. **1989**, *158*, 312. (c) Lanzani, G.; Cervllo, G.; Zavelan-Rossi, M.; De Silvestri, S. *Synth. Met.* **2001**, *116*, 1.

(31) Terenin, A.; Kobyshev, G.; Lialin, G. *Photochem. Photobiol*. **1966**, *5*, 689.

(32) Bajema, L.; Gouterman, M.; Rose, C. B. *J. Mol. Spectrosc*. **1971**, *39*, 758.

(33) (a) Janowski, A.; Rezeszotarska, J. *J. Lumin.* **1980**, *21*, 409. (b) Yoshizawa, M.; Suzuki, K.; Kubo, A.; Saikan, S. *Chem. Phys. Lett*. **1998**, *290*, 43. (c) Bhasikuttan, A C.; Okada, T. *J. Phys. Chem. A* **2003**, *107*, 3030.

(34) Ermolaev, V. L. Russ. *Chem. Rev*. **2001**, *70*, 471.

(35) Okuyama, K.; Hasegawa, T.; Ito, M.; Mikami, N. *J. Phys. Chem.* **1984**, *88*, 1711.

(36) Nemes, P.; Demeter, A.; Biczok, L.; Bereces, T.; Wintgens, V.; Valat, P.; Kossanyi, J. *J. Photochem. Photobiol., A* **1998**, *113*, 225.

(37) Wassam, W.; Lim, E. C. *J. Chem. Phys*. **1978**, *68*, 433; **1978**, *69*, 2175.

(38) Van der Burget, M. J.; Jansen, I. M. G.; Huizer, A. H.; Varma, C. A. G. O. *Chem. Phys.* **1995**, *201*, 525.

(39) (a) Anderson, P. A.; Gilbro, T.; Asato, A. E.; Liu, R. S. H. *J. Lumin.* **1992,** *51*, 11. (b) Mimuro, M.; Nagashima, U.; Nagaoka, S.; Nishimura, Y.; Takaichi, S.; Katoh, T.; Yamazaki, I. *Chem. Phys. Lett*. **1992**, *191*, 219. (c) Cosgrove, S. A.; Cuite, M. A.; Burnell, T. B.; Christensen, R. L. *J. Phys. Chem*. **1990**, *94*, 8118.

(40) Cehelnic, E. D.; Cundall, R. B.; Lockwood, J. R.; Palmer, T. F. *J. Phys. Chem.* **1975**, *79*, 1369.

(41) Lewanowicz, A.; Lipiñski, J. *J. Mol. Struct*. **1998**, *450*, 163.

(42) Atom, Y. W.; Robert, H.; Lewis, J. W.; Zangh, J. Z.; Klinger, D. S. *J. Phys. Chem. A* **1999**, *10 3*, 2388.

(43) Kukura, P.; McCamant, D. W.; Mathies, R. A. *J. Phys. Chem. A*, in press.

(44) Kramers, H. A. *Physica* **1940**, *7*, 284.

(45) Werner, A. M.; Ippen, E. P. *Chem. Phys. Lett.* **1985**, *114*, 456.

(46) Brito Cruz, C. H.; Fork, R. L.; Knox, W. H.; Shank, C. V. *Chem. Phys. Lett.* **1986**, *132*, 341.

(47) Wild, W.; Seilmeier, A.; Gottfried, N. H.; Kaiser, W. *Chem. Phys. Lett.* **1985**, *119*, 259.

(48) Martini, I.; Hartland, G. V. *J. Phys. Chem.* **1996**, *100*, 19764.

(49) Bertolini, D.; Cassettari, M.; Salvetti, G. *J. Chem. Phys.* **1982**, *76*, 325.

(50) Garg, S. K.; Smyth, C. P. *J. Phys. Chem.* **1965**, *69*, 1294.

(51) Riddick, J. A.; Bunger, W. B. *Organic Solvents*, 3rd ed.; Wiley: New York, 1970.

(52) Simon, J. D. *Acc. Chem. Res.* **1988**, *21*, 128.

(53) Horng, H. L.; Dahl, K.; Jones, G., II; Maroncelli, M. *Chem. Phys. Lett.* **1999**, *315*, 363.